

# Synchronization Phenomena of Chaotic Map Lattice with Time Varying Coupling

Yoko Uwate  
and Yoshifumi Nishio

Dept. of Electrical and Electronics Engineering,  
Tokushima University, Japan,  
phone: +81-88-656-7470; fax: +81-88-656-7471;  
email: {uwate, nishio}@ee.tokushima-u.ac.jp.

Ruedi Stoop

Institute of Neuroinformatics,  
University / ETH Zurich, Switzerland,  
email: ruedi@ini.phys.ethz.ch  
http://stoop.ini.unizh.ch/

**Abstract**—Synchronization phenomena based upon of globally coupled maps are studied in many fields of natural science. In this contribution, we study synchronization phenomena in chaotic map lattices with time varying couplings. By computer simulations, we confirm the presence of the switching synchronization.

## I. INTRODUCTION

Coupled chaotic systems are good models to describe various higher-dimensional nonlinear phenomena occurring in natural science. Figure 1 shows a set of globally coupled maps (GCM) and the coupled map lattice (CML) proposed by Kaneko and Bunimovich [1]- [5]. Whereas in the CML, each cell connects to only adjacent cells, the cells of the GCM are connected globally. Both models are able to generate complex patterns [7]- [9].

There are, however, systems for which the dissipation factors vary with time, e.g. if the dissipation is dependent on changing ambient temperature, for an equation describing an object moving in a space with local friction, or in the case of a circuit with a resistor the temperature coefficient of which is sensitive, such as a thermistor. Despite, GCM with time-varying couplings have only been addressed by a small number of studies.

In the present contribution we investigate synchronization phenomena of GCM with time varying couplings. We implement the time varying coupling by switching of the sign of the coupling strength. By computer simulations, the switching synchronization of this system can be evidenced.

## II. COUPLED CHAOTIC MAP

### A. Chaotic map

The equation of the GML is defined as follows: Each cell is connected to 4 next neighboring cells following in its time evolution the equation

$$x_{ij} = (1 - \varepsilon)f(x_{ij}(t)) \pm \frac{\varepsilon}{4} \sum_{kl \in \Xi_1} f(x_{kl}(t)), \quad (1)$$

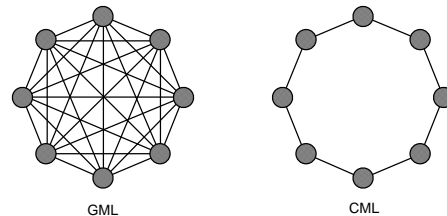


Fig. 1. Network model.

where  $\varepsilon$  is coupling strength,  $t$  denotes the number of iterations and  $i, j$  is the index of the cell considered.

As a simple example, we use the logistic map as simple chaotic site map  $f$ . The equation of the logistic map is defined as

$$f(x) = \alpha x(1 - x) \quad (2)$$

where  $\alpha$  is the so-called bifurcation parameter, ruling the degree on nonlinearity. A graph of this map is shown in Fig. 2, for  $\alpha = 4$ .

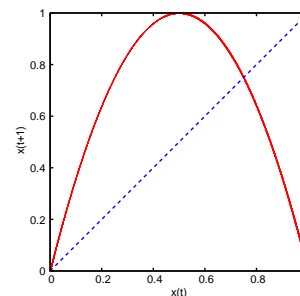


Fig. 2. Logistic Map.

### B. Definition of synchronization

Synchronization in the described system is defined as follows. We compare  $x_{ij}$  to the average of the 4 neighboring

cells. We will say that the cell synchronizes with its neighbors if

$$|x_{ij} - \frac{1}{4} \sum_{kl \in \Xi_1} x_{kl}| < 0.03. \quad (3)$$

is satisfied.

### III. SIMULATED RESULTS

For our simulations, we investigated the behavior of this synchronization measure on a grid of 50x50 cells, with fixed values ( $\epsilon=0.5$ ) on the boundary. Initial conditions for the cells were otherwise random, uniformly distributed on the unit interval.

#### A. Positive Coupling

Figure 3 shows snapshots of computer simulations. In this figure, blue (dark) boxes indicate cells that synchronize with their neighbors, whereas white boxes indicate lack of synchronization. At the beginning ( $t=1$ ) most cells are not synchronized with their neighborhood, already after short time ( $t=10$ ), the synchronized cells dominate. The effect can be captured by the ratio of synchronization evaluated across the time evolution, for different values of the nonlinearity parameter  $\alpha$ , see Fig. 4, demonstrating the dramatic effect this parameter has on synchronization. In the case of  $\alpha = 2.8$  (leading to period-1 solutions of the site map), the ratio of synchronization rapidly changes from low to high, in the case of  $\alpha=3.99$  (corresponding to fully-developed chaotic site maps) the cells remain essentially unsynchronized.

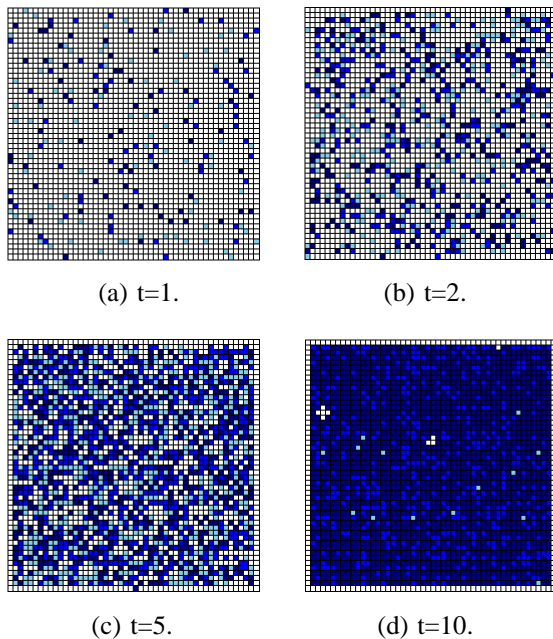


Fig. 3. Snapshots of simulations ( $\alpha=2.8$ ,  $\epsilon=0.25$ ).

Next, we investigate how the synchronization measure depends on the nonlinearity parameter  $\alpha$  of the chaotic map. When the uncoupled site map is on period-1 solutions, the ratio of synchronized cells is around 90 percent. At the point of

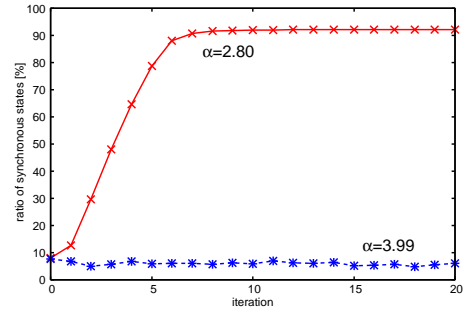


Fig. 4. Evolution of the synchronization measure (percentage of synchronized cells, averaged over 100 trials).

changing from period-1 to period-2 solution, synchronization decreases sharply, until it remains almost constant, around 10 percent. Figure 6 shows the synchronization upon variations of  $\alpha$  and  $\epsilon$ . From this figure, we infer that the influence of  $\epsilon$  on synchronization in the situations considered, is negligible.

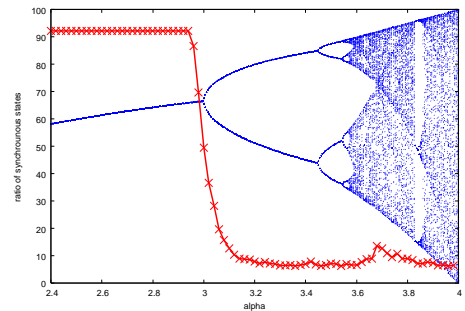


Fig. 5. Synchronization as a function of  $\alpha$ .

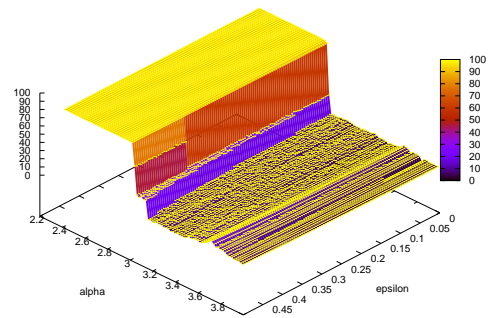


Fig. 6. Synchronization as a function of  $\alpha$  and  $\epsilon$ .

#### B. Negative Coupling

Next, we consider the case of chaotic maps coupled by means of negative factors. Figure 7 shows the dependence of synchronization on the nonlinearity parameter  $\alpha$ . In the case of  $\alpha = 2.8$ , the synchronization measure is zero. In the case of  $\alpha = 3.99$ , the synchronization measure stays around 5 percent.

Figure 8 Synchronization mediated by negative coupling, as a function of the nonlinearity parameter  $\alpha$ , demonstrating the lack of synchronization. We also evaluated the synchronization measure as a function of the parameters  $\alpha$  and  $\varepsilon$ , see Fig. 9. The ratio of synchronization state in almost everywhere shows around zero. In the condition of negative coupling, cells are dis-synchronous with neighboring cells, as the negative coupling works against synchronization.

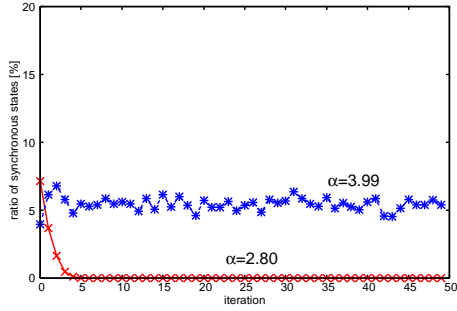


Fig. 7. Synchronization as a function of time.

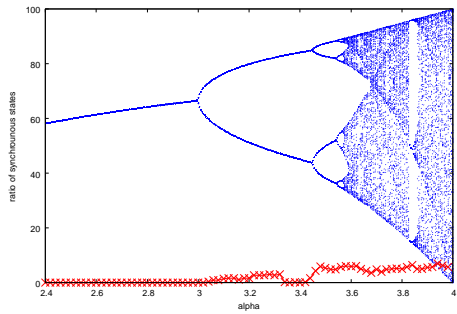


Fig. 8. Synchronization as a function of the site nonlinearity  $\alpha$ .

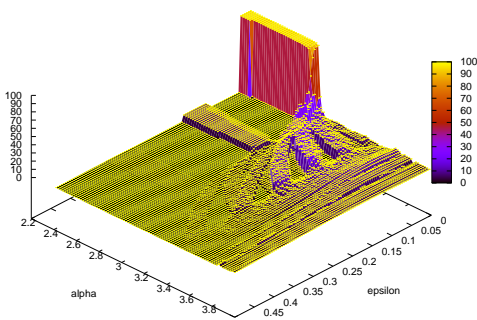


Fig. 9. Synchronization as a function of  $\alpha$  and  $\varepsilon$ .

### C. Switching Coupling

Finally, we apply time varying coupling in the form of periodically switching coupling, where the switching periods are held fixed at 50 iteration. The simulation results are

shown in Figs. 10-14. Figure 10 shows the simulation results obtained for the site nonlinearity parameter  $\alpha = 2.8$ . In this case, the uncoupled logistic maps are on period-1 solutions. From this figure, we confirm that the ratio of synchronization states switches between slightly above zero and about 90 percent. If the nonlinearity parameter is varied, a behavior of the synchronization measure as demonstrated in Figures 11-14 (a) is obtained, where the nonlinearity parameter  $\alpha$  is increased across the set  $\{3.3, 3.84, 3.54, 3.99\}$ . In these cases, the behavior of the uncoupled logistic map is period-2, period-3, period-4 and fully developed chaos, respectively. In this case, by zooming in into the more global synchronization behavior, more complex local switching patterns are observed, see Figs 11-14 (b). From these figures, we can see that the synchronization measure also oscillates with period-2, period-3, period-4, and chaotically.

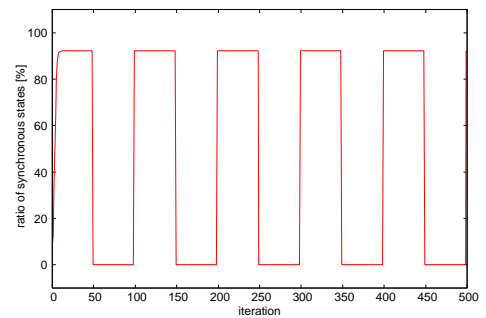
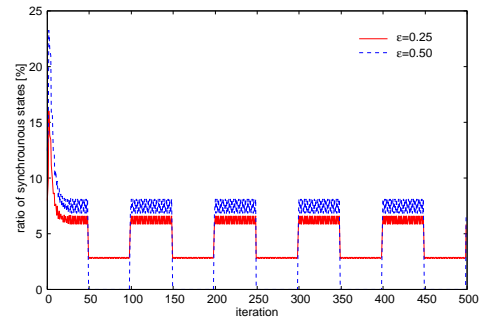
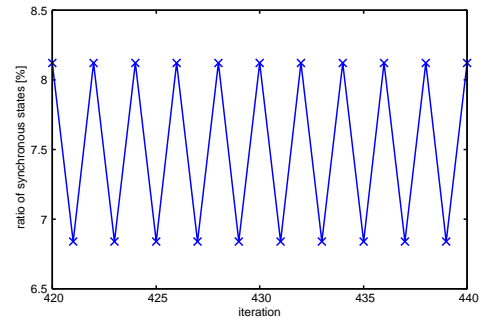


Fig. 10. Switching synchronization (parameters:  $\alpha=2.8$ ,  $\varepsilon=0.25$ ).

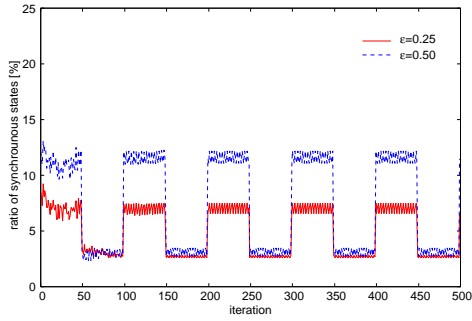


(a) Switching synchronization.

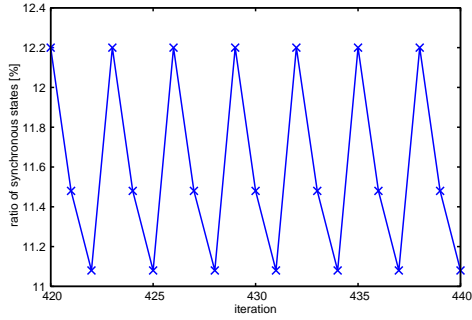


(b) Zooming in: Period-2 oscillation.

Fig. 11. Switching synchronization obtained for  $\alpha = 3.3$ .



(a) Switching synchronization.



(b) Zooming in: Period-3 oscillation.

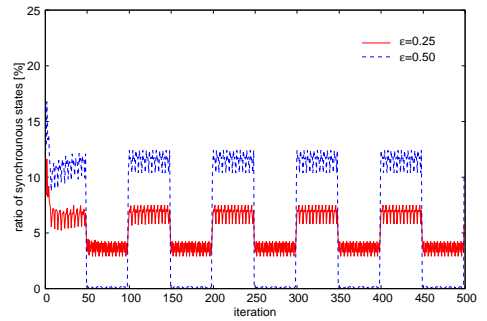
Fig. 12. Switching synchronization obtained for  $\alpha = 3.84$ .

#### IV. CONCLUSION

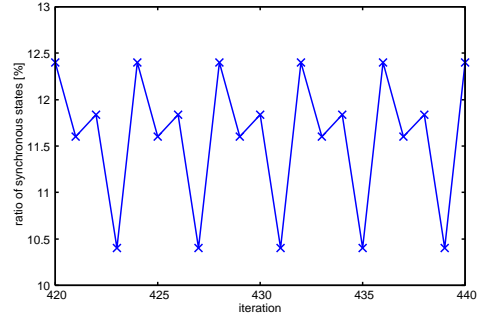
In this study, we have investigated the synchronization phenomena of GCM with time varying coupling. We implement the time varying coupling by switching the sign of the coupling strength. By computer simulations, the switching synchronization of this system could be confirmed.

#### REFERENCES

- [1] K. Kaneko, "Spatiotemporal Intermittency in Coupled Map Lattice," *Prog. Theor. Phys.*, vol.75, no.5, pp.1033-1044, 1985.
- [2] L. A. Bunimovich and Ya. G. Sinai, "Spacetime Chaos in Coupled Map Lattices," *Nonlinearity* 1, no.4, pp.491-516, 1988.
- [3] K. Kaneko, "Pattern Dynamics in Spatiotemporal Chaos," *Physica D*, vol.34, pp.1-41, 1989.
- [4] K. Kaneko, "Spatiotemporal Chaos in One- and Two- Dimensional Coupled Map Lattice," *Physica D*, vol.37, pp.60-82, 1989.
- [5] K. Kaneko, "Simulating Physics with Coupled Map Lattice - Pattern Dynamics, Information Flow, and Thermodynamics of Spatiotemporal Chaos," *Formation, Dynamics, and Statistics of Patterns*, World Sci., pp.1-52, 1990.
- [6] Y. Nishio and A. Ushida, "Spatio-Temporal Chaos in Simple Coupled Chaotic Circuits," *IEEE Trans. on Circuit and Systems-I*, vol.42, no.10, pp.678-686, 1995.
- [7] M. Wada, K. Hirai and Y. Nishio, "A Mult-Agent System and State Control of Coupled Chaotic Maps," *Proc. of NOLTA'01*, vol.1, pp.211-214, 2001.
- [8] K. Kitatsuji and M. Wada, "Spatio-temporal Chaos and Several Phase Patterns in Coupled Chaotic Maps using Fifth-Power Function," *Proc. of NCSP'05*, pp.113-116 2005.
- [9] M. Wada, K. Kitatsuji and Y. Nishio, "Spatio-temporal Phase Patterns in Coupled Chaotic Maps with Parameter Deviations," *Proc of NOLTA'05*, pp.178-181 2005.

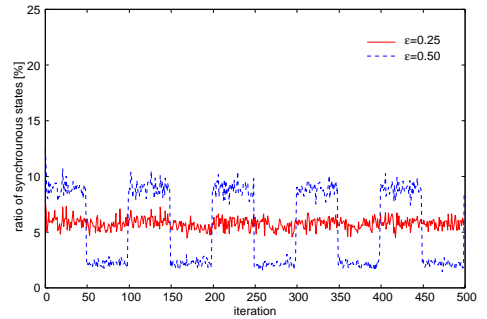


(a) Switching synchronization.

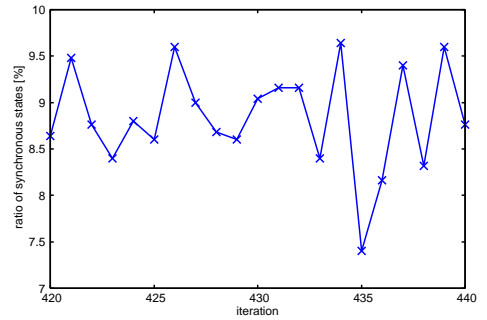


(b) Zooming in: Period-4 oscillation.

Fig. 13. Switching synchronization obtained for  $\alpha = 3.54$ .



(a) Switching synchronization.



(b) Zooming in: Chaotic oscillation.

Fig. 14. Switching synchronization obtained for  $\alpha = 3.99$ .